Journal of Oceanography
https://doi.org/10.1007/s10872-018-0476-y

SHORT CONTRIBUTION

# Observations of intraseasonal variability in the Sunda Strait throughflow

**Shujiang Li[1,2] · Zexun Wei[1,2] · R. Dwi Susanto[3,4] · Yaohua Zhu[1,2] · Agus Setiawan[5] · Tengfei Xu[1,2] · Bin Fan[1,2] · Teguh Agustiadi[5] · Mukti Trenggono[6] · Guohong Fang[1,2]**

Received: 30 November 2017 / Revised: 16 April 2018 / Accepted: 18 April 2018


**Abstract**
Using velocity profiles observed by bottom-mounted ADCPs, we identified strong intraseasonal variability in the Sunda Strait throughflow. This intraseasonal variability, with typical periods of 20–40 days and the strongest energy occurring in the boreal spring, can reverse the Sunda Strait throughflow. Further analysis showed this intraseasonal variability to be closely related to local zonal wind and the sea level gradient along the strait. These observations confirm for the first time the existence of Kelvin-wave-like signals in the Sunda Strait, propagating from the equatorial Indian Ocean. This study also provides new insights into the effects of Kelvin waves on the Sunda Strait throughflow.

**Keywords** Sunda Strait throughflow · Intraseasonal variability · Zonal winds · Sea level anomalies · Kelvin waves

## 1 Introduction

The Sunda Strait separates the Indonesian islands of Java and Sumatra, and it connects the Java Sea to the Indian Ocean (Fig. 1a). At its narrowest, the Sunda Strait is only 18 km in width. A small island (Sangeang Island) splits the northern end of the Sunda Strait into two channels; the western channel has a maximum depth of 98 m, and the eastern channel has a maximum depth of 70 m. As it is the westernmost exit from the Lesser Sunda Islands, the Sunda Strait is an important outflow passage of the Indonesian Throughflow (ITF) (Susanto et al. 2016).

Over the past several decades, extensive studies have been carried out on the ITF and the regional oceanography in the Indonesian Seas. In particular, significant seasonal and intraseasonal oceanic signals have been revealed in the main inflow passage of the ITF, the Makassar Strait, and its major outflow passages, including the Lombok Strait, the Ombai Strait, and the Timor Passage, using in situ measurements (Dharma and Murray 1996; Molcard et al. 1996; Susanto et al. 2000; Wijffels and Meyers 2004) and satellite data (Iskandar et al. 2005). Also, as part of the International Nusantara Stratification and Transport (INSTANT) program, the intraseasonal variability (ISV) of the ITF has been investigated (Sprintall et al. 2009; Pujiana et al. 2013; Gordon et al. 2010; Drushka et al. 2010).

Due to a lack of observations, the variability of the ITF outflow in the Sunda Strait is not well known. Susanto et al. (2016) noted that seasonal reversal of low-salinity transport in the Sunda Strait plays an important role in water exchange between the Pacific and Indian Oceans. However, the existence of ISV in the Sunda Strait throughflow has not been reported in the literature. Based on recent observations, here we report the identification of strong ISV in the Sunda Strait throughflow. Further analyses of the data reveal new

✉ Zexun Wei
weizx@fio.org.cn

1 Key Laboratory of Marine Science and Numerical Modeling, First Institute of Oceanography, State Oceanic Administration, 6 Xianxialing Road, Laoshan District, Qingdao 266061, China

2 Laboratory for Regional Oceanography and Numerical Modeling, Qingdao National Laboratory for Marine Science and Technology, Qingdao, China

3 Department of Atmospheric and Oceanic Science, University of Maryland, College Park, USA

4 Faculty of Earth Sciences and Technology, Bandung Institute of Technology, Bandung, Indonesia

5 Agency for Marine & Fisheries Research, Ministry of Marine Affairs and Fisheries, Jakarta, Indonesia

6 Department of Marine Science, Faculty of Fisheries and Marine Science, Jenderal Soedirman University, Purwokerto, Indonesia

Published online: 14 May 2018

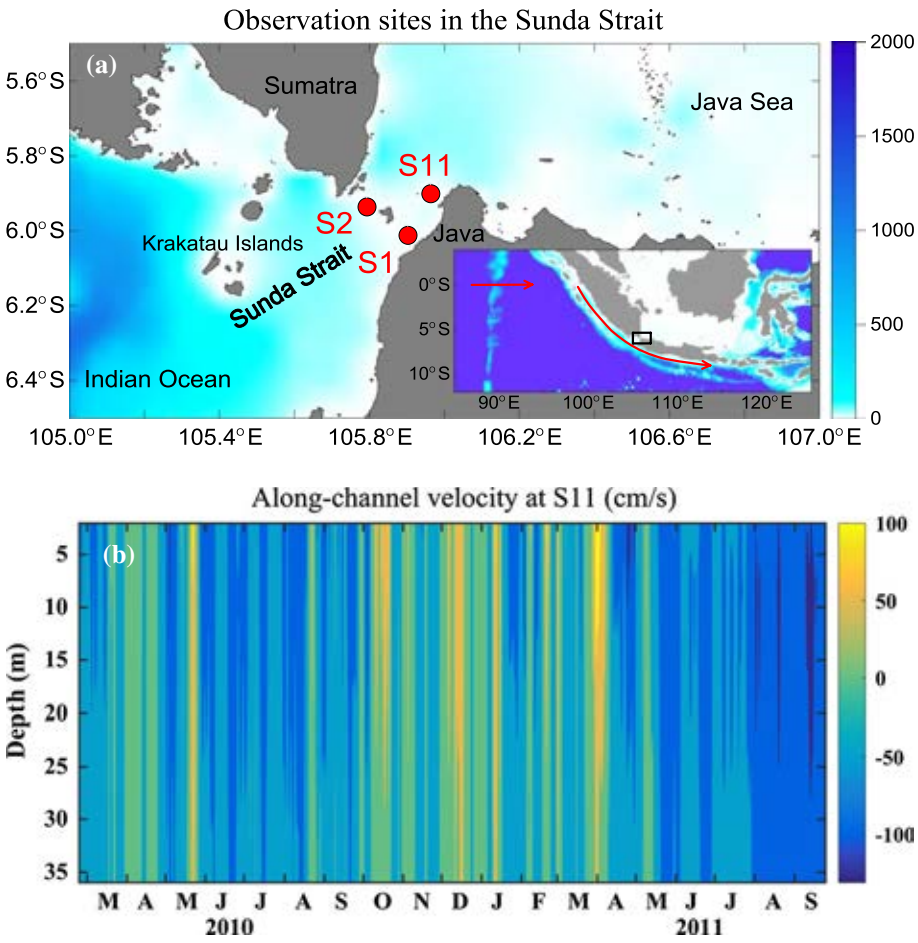


**Fig. 1** **a** Observation sites in the Sunda Strait and **b** the along-channel velocity at S11. In Fig. 1a, the *bottom right panel* shows the location of the Sunda Strait and a schematic of the Kelvin waveguide, redrawn based on Schiller et al. (2010) and Iskandar et al. (2014)

characteristics of this ISV and its associated dynamics along the south coast of Sumatra–Java.

## 2 Data and methods of analysis

To make the first direct, full-depth current measurements of the Sunda Strait throughflow, the South China Sea-Indonesian Seas Transport/Exchange (SITE) and Impacts on Seasonal Fish Migration program was established jointly by scientists from China, Indonesia, and the United States in October 2006 (Fang et al. 2010; Susanto et al. 2013, 2016; Wei et al. 2016). In this program, we deployed trawl-resistant bottom mounts (TRBMs) equipped with acoustic Doppler current profilers (ADCPs) and bottom conductivity-temperature-depth (CTD) loggers to obtain both current profiles and water properties in the Sunda Strait. This study employs data from three stations (Fig. 1) located in the major passages of the Sunda Strait. Stations S1 (105°54.08′E, 6°0.79′S) and S2 (105°47.51′E, 5°56.22′S) are located in the two channels on each side of Sangeang Island in the northern Sunda Strait at water depths of 55.3 m and 97.6 m, respectively. The TRBMs were deployed at S1 and S2 on November 9, 2008 and recovered on October 20, 2009 and July 20, 2009, respectively. The TRBM was deployed at S11 (105°57.75′E, 5°54.09′S) in the northern Sunda Strait on February 23, 2010 and recovered on September 25, 2011. Current observations were made at this station, which has a water depth of 37 m, for the longest period (20 months). All three of the TRBMs included an upward-looking, self-contained, 300-kHz ADCP deployed on the seabed. The bin size and sampling interval of the ADCPs were set to 2 m and 20 min, respectively.

The strong tidal current in the Sunda Strait was removed using a low-pass filter with a cutoff period of 48 h before the data were analyzed. The daily subtidal velocity was decomposed into along-channel and cross-channel components (Fang et al. 2010; Susanto et al. 2016). Because it is constrained by the narrow channel, the current in the Sunda Strait is dominated by the along-channel component, which is oriented approximately 40° relative to true north. The subtidal currents at the three stations show similar vertical structures from the surface to the bottom (Fig. 1b for S11; Fig. 6 from Susanto et al. 2016 for S1 and S2), suggesting that the flow in the Sunda Strait is quasi-barotropic, and the correlation coefficients between the different levels are all greater than 0.94. In order to study the ISV of the Sunda

Strait throughflow, we obtained the time series of vertical mean along-channel velocities for further analysis. To study the structure and development of spectra, we employed the ensemble empirical mode decomposition (EEMD) method, which is widely used in geophysics (Wu and Huang 2009).

A 20–90-day Butterworth filter was employed to analyze the ISV in the along-channel velocities. The data on sea surface wind at 10 m used in this work were from the cross-calibrated multi-platform (CCMP) V2.0 data set (Atlas et al. 2011). These data are daily averages, and the data set has a horizontal resolution of 0.25° × 0.25°. The daily-averaged sea-level anomaly (SLA) data are produced by Ssalto/Duacs and distributed by Archiving, Validation, and Interpretation of Satellite Oceanographic Data (AVISO), and this data set has a horizontal resolution of 0.25° × 0.25° (Ducet et al. 2000).

## 3 Results

### 3.1 General features of the ISV

#### 3.1.1 Strength

The results of 20–90-day band-pass filtering reveal strong ISV in the Sunda Strait throughflow (Fig. 2a–c). At S1, S2, and S11, the intraseasonal signal ranges of 91, 93, and 120 cm/s are significantly greater than the seasonal signal ranges of 83, 59, and 101 cm/s, respectively. The ISV accounts for 59%, 35%, and 47% of the total subtidal current variance at these three stations, respectively, showing the important role of the ISV in regulating the variability in the Sunda Strait throughflow. Although long-term mean volume transport of the intraseasonal current is zero, the frequent reversal of the current contributes to the development of different water properties within the Java Sea and Indian Ocean, which lie at opposite ends of the Sunda Strait. The intraseasonal exchange rate can be estimated as $E_v = \int_A |v| dA$. In this formula, the integration is performed along the cross-section, and $v$ and $dA$ denote the intraseasonal along-channel current and the area element of the cross-section, respectively. During the period of observations at S11 (2010–2011), the annual mean intraseasonal exchange rate in the Sunda Strait was $0.26 \pm 0.17$ Sv ($1\ \text{Sv} = 10^6\ \text{m}^3\ \text{s}^{-1}$). This value is comparable to the seasonal exchange rate of $0.34 \pm 0.15$ Sv, suggesting that the ISV makes an important contribution to the water exchange between the Java Sea and Indian Ocean.

Given the existence of the ISV, the Sunda Strait throughflow reverses its direction rather frequently, particularly in boreal winter and spring (Fig. 2a–c). The reversal in current direction greatly enhances the water exchange between the Indian Ocean and Java Sea. The observed maximum velocity of the ISV in the Sunda Strait was 82 cm/s in April

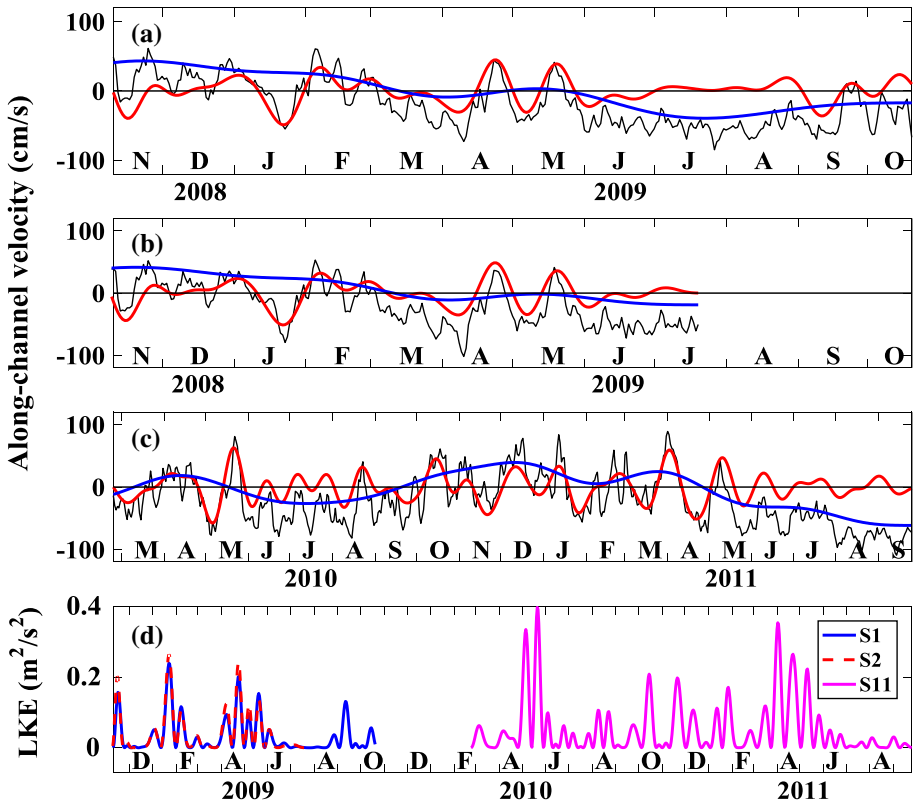


**Fig. 2a–c** Time series of vertically averaged along-channel velocities at **a** S1, **b** S2, and **c** S11. **d** Time series of the low-frequency kinetic energy (LKE) at these stations in the Sunda Strait. In panels **a**, **b**, and **c**, the *black lines* indicate the daily mean values; the *red lines* indicate the intraseasonal variation after 20–90-day bandpass filtering; and the *blue lines* indicate the seasonal variation after 90-day low-pass filtering. The annual means (−17, −25 and −18 cm/s at S1, S2, and S11, respectively) are removed before plotting. Positive/negative values represent inflow/outflow into/from the Java Sea along the channel

2011, which is greater than the corresponding values of 50–60 cm/s observed in other ITF passages (Iskandar et al. 2014; Zhou and Murtugudde 2010).

### 3.1.2 Spectrum

To isolate the different timescales, the time series of vertically averaged along-channel velocities were analyzed using the EEMD spectral analysis method of Wu and Huang (2009). Hilbert spectrum results obtained by applying the EEMD to the time series observed at S1, S2, and S11 show rich spectra at the intraseasonal scale (Fig. 3). All of the observations contain a peak in the power at periods of 20–40 days, i.e., in the relatively high-frequency section of the intraseasonal spectral band (20–90 days). The ISV with 20–40-day periods accounts for most of the energy in each spectrum, and two maxima occur at periods of 26–28 and 37 days. The energy density reaches its maximum with a period of 24–28 days at S1 and S2 in spring 2009 and with a period of about 40 days at S11 in spring 2011.

### 3.1.3 Seasonality of the ISV

Figure 2 illustrates that the ISV of the Sunda Strait throughflow undergoes a seasonal cycle. Strong ISV events occur throughout the year, except in boreal summer. The maximum velocities of the ISV occur primarily during the monsoon transition and northwesterly monsoon season, in boreal spring and winter, respectively. To evaluate this seasonal variability of ISV, the low-frequency kinetic energy (LKE) was calculated as $\mathrm{LKE} = (u^2 + v^2)/2$. Here, $u$ and $v$ represent the cross- and along-channel intraseasonal velocities, respectively. The result (Fig. 2d) shows a distinctive seasonal cycle in the ISV. Over the entire period of observations, the primary peak in the LKE occurs during the monsoon transition season in boreal spring, whereas the secondary peak occurs during the northwesterly monsoon season in boreal winter. The ISV is relatively inactive in boreal summer.

The EEMD results (Fig. 3a–c) also confirm the seasonal characteristics of the ISV with periods of 20–40 days. The primary peak season of the ISV occurs in April/May during the monsoon transition, and the secondary peak season occurs in boreal winter when the northwest monsoon prevails; however, the ISV is in an inactive phase in boreal summer during the southeast monsoon, which means that the southeast monsoon suppresses the ISV in the Sunda Strait throughflow. The results also indicate that the Sunda Strait throughflow includes the ISV located in the relatively low-frequency section (40–90 days) of the intraseasonal spectral band. However, this relatively low-frequency ISV is weaker and occurs less frequently than the ISV of the high-frequency section.

These seasonal features (specifically, an active phase in boreal winter and an inactive phase in boreal summer) coincide with those of the Madden–Julian Oscillation (MJO) (Madden and Julian 1994), which implies that the ISV in the Sunda Strait throughflow may be related to the MJO in the Indian Ocean. The primary peak that occurs in boreal spring seems to be due to a different mechanism; it is most likely related to the propagation of Kelvin waves along the

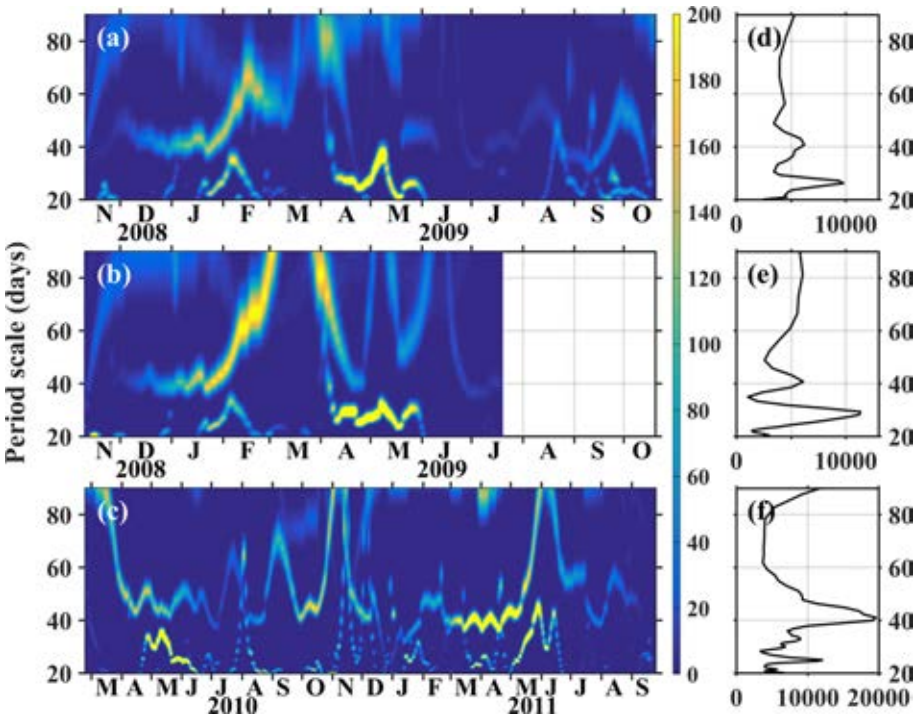


**Fig. 3** Hilbert spectra at the intraseasonal scale, derived by applying the EEMD method to the time series at S1 (Fig. 3a, d), S2 (Fig. 3b, e), and S11 (Fig. 3c, f)

southwest coast of Sumatra–Java. The details are discussed below.

### 3.2 The local forces of the ISV

Based on the band-passed along-channel throughflow, we defined the inflow/outflow peaks, with ISV amplitudes greater than 30 cm/s as positive/negative ISV events ($+v'/-v'$). There were 10 $+v'$ and 12 $-v'$ events during the period of observations, and each event lasted for about one month. On average, 3.3, 1.0, 2.0, and 2.5 ISV events occurred in boreal spring, summer, autumn, and winter, respectively, in one seasonal cycle. This result indicates that the ISV in the Sunda Strait throughflow occurs more frequently in boreal spring than in other seasons. A composite analysis was performed to explore the characteristics and evolution of these ISV events. The mean duration of the 22 ISV events was found to be approximately 30 days, consistent with the results from spectral analysis. In the subsequent analysis, we divided one life cycle of each ISV event into five phases, with each phase lasting a duration of 7 days. The 7-day mean intraseasonal SLA and intraseasonal sea surface winds for each phase were calculated to produce the composite diagrams shown in Fig. 4.

Figure 4 shows that the sea level gradients between the two sides of the Sunda Strait produced by the SLAs and the intraseasonal sea surface winds correlate well with the flow phases. During phase I of the $+v'$ events, easterly wind anomalies are present over the Sunda Strait that drive the surface water to flow against the north side but away from the south side of the Java Island, inducing a sea level gradient pointing toward the Indian Ocean. This sea level gradient favors a net outflow into the Sunda Strait that further enhances the ITF transport (Fig. 4a). Weak westerly wind anomalies begin to develop during phase II, accompanied by a near-flat sea level in the Sunda Strait, resulting in insignificant throughflow in the strait (Fig. 4b). Phase III is the mature phase of the $+v'$ events, and this phase features a positive SLA along the southwest coast of Sumatra–Java and a negative SLA in the Java Sea (Fig. 4c). This SLA distribution is partly attributable to strong westerly wind anomalies that drive on/offshore water transport on the Indian Ocean (box on the left in Fig. 4a)/Java Sea (box on the right in Fig. 4a) side of the Sunda Strait. The Sunda Strait throughflow weakens in phase IV, consistent with the decay in westerly wind anomalies and the sea level gradient (Fig. 4d). Easterly wind anomalies develop in phase V, driving off/onshore water transport on the Indian Ocean/Java Sea side of the Sunda Strait that is favorable to a southward sea-level gradient and thus a net outflow in the strait (Fig. 4e). The evolution of the $-v'$ events is opposite to that of the $+v'$ events (Fig. 4f–j), in which both the Ekman and

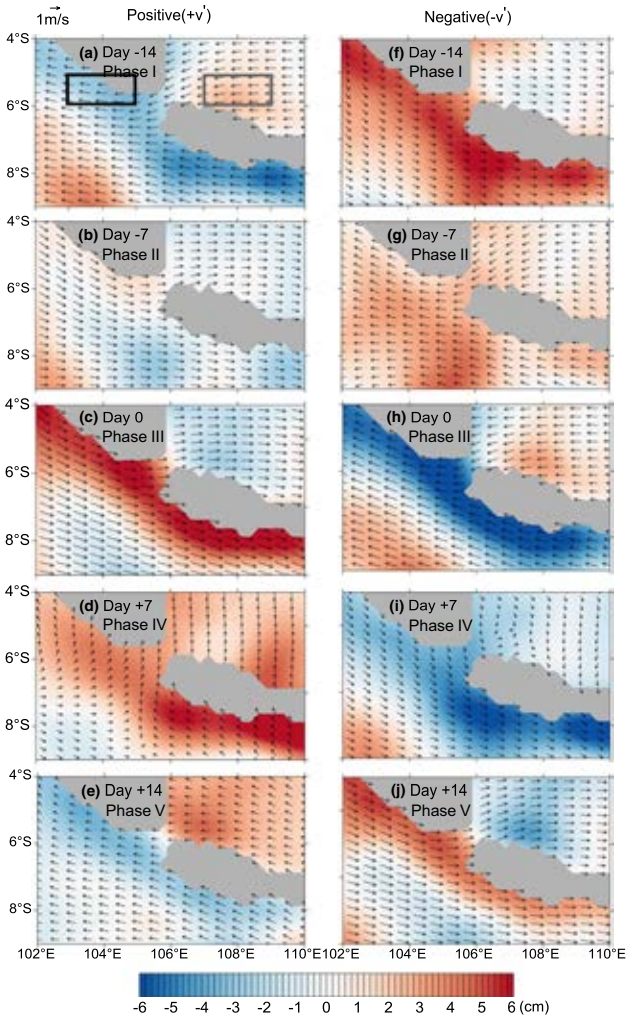


**Fig. 4a–j** Composite intraseasonal sea level anomalies (*shading*) and surface wind anomalies (*vectors*) for phase I through V of the positive (**a**–**e**) and negative (**f**–**j**) ISV events in the Sunda Strait throughflow. Day 0 (phase III) indicates the peak of the ISV events, with northward/southward intraseasonal flow occurring from the Indian Ocean/Java Sea to the Java Sea/Indian Ocean for the positive/negative ISV events, respectively. The sea level gradient across the Sunda Strait was calculated with reference to the sea level difference between 103–105°E, 6–5°S (*box on the left* in **a**) and 107–109°E, 6–5°S (*box on the right* in **a**)

sea-level-driven currents forced by the reversed intraseasonal winds play leading roles.

The maximum correlation coefficient between the local zonal winds (105°E–107°E, 7°S–5°S) and the currents is 0.78 (+2) at the intraseasonal scale. Here, the number in parentheses indicates the number of days by which the local zonal wind leads the current. We selected two typical regions (103–105°E, 6–5°S and 107–109°E, 6–5°S) to use to calculate the sea level gradient across the Sunda Strait; the correlation coefficient between this gradient and the along-channel velocity reaches 0.82 (0) at the intraseasonal scale. During the mature phase of the ISV events, the SLA along

the southwest coast of Sumatra–Java shows strong variability, and the maximum of these anomalies exceeds 6 cm. This variability is much stronger than that on the Java Sea side. This asymmetry implies that other processes influence the SLA along the southwest coast of Sumatra–Java. The propagation of coastal Kelvin waves is an example of these processes (Xu et al. 2016). The details are examined below.

### 3.3 Remote sources of the ISV

The origin of the ISV observed in the Sunda Strait can be traced to the equatorial Indian Ocean. We composited the SLAs and zonal wind anomalies based on 22 ISV events in the Sunda Strait throughflow. The 20–90-day bandpass-filtered zonal wind anomalies were averaged longitudinally over 10°S–10°N, and the 20–90-day band-passed SLAs along the equator and the south coast of Sumatra-Java were selected (red line in Fig. 1a). For convenience, the zonal wind anomalies and SLAs were multiplied by −1 for the negative ISV events.

The composite time–longitude plot in Fig. 5a shows that the intraseasonal zonal wind anomaly originates from as far away as 75°E in the central equatorial Indian Ocean. During an ISV event, a zonal wind anomaly with a typical period of 20–40 days propagates eastward along the equator. As this anomaly propagates eastward, the ISV of the zonal wind anomaly reaches its maximum strength near 80°E and weakens rapidly upon approaching the Maritime Continent. The ISV of the Sunda Strait throughflow peaks two days after the arrival of the zonal wind anomaly, consistent with the results of the leading/lag relationship between the local zonal winds and currents (Sect. 3.2). As with the zonal wind anomaly, the intraseasonal SLA signal with periods of 20–40 days can be traced as far west as 90°E in the equatorial Indian Ocean (Fig. 5b). In contrast to the zonal wind anomaly, the intraseasonal SLA becomes stronger as it propagates along the equatorial Indian Ocean and the southwest coast of Sumatra–Java. It arrives at the Sunda Strait two days after the peak of the ISV in the Sunda Strait throughflow. The intraseasonal SLA signals in the Sunda Strait are on the order of 5 cm.

The Radon transform indicates that the average phase speeds of the zonal wind anomaly and SLA are 7.37 and 3.51 m/s, respectively, which match the characteristics of Kelvin waves in the atmosphere and ocean (Roundy and Kiladis 2006). The composite analysis also shows that there are significant inverse phases between the zonal wind anomaly and SLA, both of which propagate eastward to the Sunda Strait before/after the ISV events, consistent with the local ISV evolution in the Sunda Strait (Fig. 4). Therefore, the ISV events display wave behavior, and the strength of the inverse signal before the ISV events is stronger than that after the ISV events. Based on the Radon transform, the mean periods of intraseasonal zonal wind anomalies and SLA are 32 and 23 days, respectively.

## 4 Summary and discussion

The Sunda Strait provides the first gap along the intraseasonal Kelvin waveguide that allows Kelvin waves to propagate into the Indonesian seas. The annual mean transport in the Sunda Strait is estimated to be −0.24 ± 0.53 Sv. This

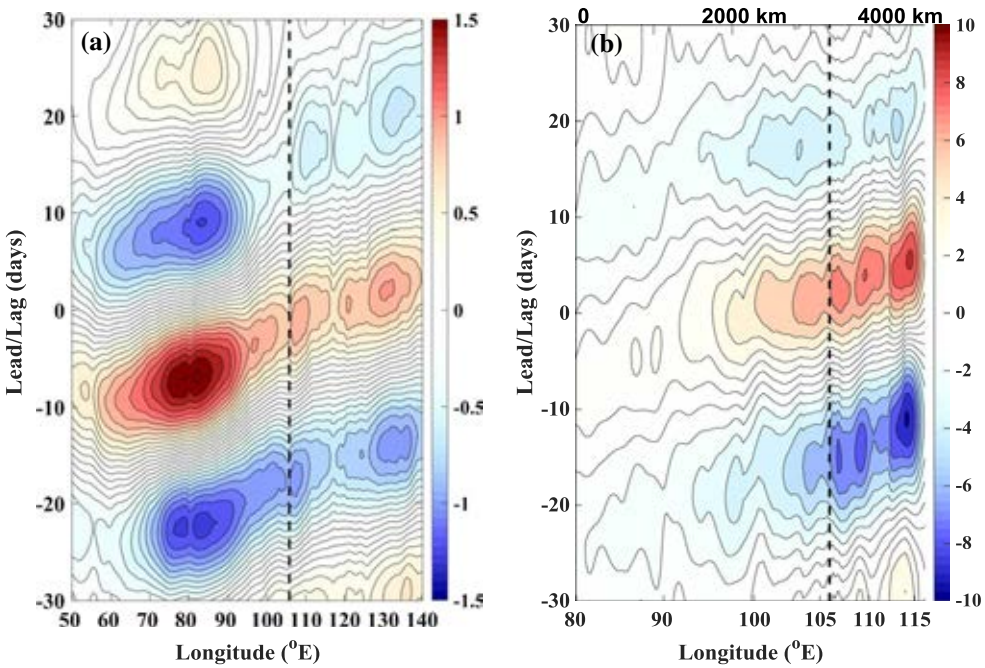


**Fig. 5** **a** Composite time–longitude plots of the 10-m intraseasonal zonal wind anomaly averaged longitudinally over 10°S–10°N and **b** the intraseasonal SLA along the equator and the south coast of the Sumatra–Java Islands during significant ISV events. Day 0 represents the peaks of the ISV events. The *dashed line* represents the location of the Sunda Strait

value is approximately one-third of the transport in the Karimata Strait, so the Sunda Strait is an important outflow channel of the ITF. The standard deviation is greater than its annual mean value, indicating that the intraseasonal variability has a strong effect on the Sunda Strait throughflow.

Based on in situ observations, this study further reveals that the Sunda Strait throughflow is subject to strong ISV with periods of 20–40 days. This ISV undergoes a distinctive seasonal cycle: it is relatively active in boreal spring and winter and is substantially suppressed in boreal summer. The seasonality of the ISV needs to be confirmed based on longer observations in order to avoid interference from interannual changes such as the El Niño/Southern Oscillation (ENSO) and the Indian Ocean Dipole (IOD). The importance of the ISV in the Sunda Strait throughflow lies in the fact that the strength of the ISV is comparable to that of the seasonal variability, so it is capable of reversing the direction of the Sunda Strait throughflow. Therefore, the ISV events enhance the water exchange between the Indian Ocean and western Java Sea.

The ISV in the Sunda Strait throughflow is forced mainly by zonal wind anomalies and SLAs, both of which originate in the equatorial Indian Ocean. The strength of the ISV on the Indian Ocean side is greater than that on the Java Sea side, implying a possible contribution to the SLAs from coastal Kelvin waves along the southwest coast of Sumatra–Java. The different roles played by local effects and coastal Kelvin waves in forcing the ISV of the Sunda Strait throughflow require further investigation.

**Acknowledgements** The Chinese researchers are supported by the National Natural Science Foundation of China (grants no. 41306031, 41476025, and 41506036), the NSFC-Shandong Joint Fund for Marine Science Research Centers (grant no. U1606405), the National Program on Global Change and Air-Sea Interaction (grant no. GASI-IPOVAI-01-02, GASI-IPOVAI-02 and GASI-IPOVAI-03), the Basic Research Operating Funds of the First Institute of Oceanography, State Oceanic Administration (grant no. 2013G35 and 2014G26), and the China Postdoctoral Science Foundation (grant no. 2014M561883). The Indonesian researchers are supported by the Agency for Marine and Fisheries Research and Human Resources. The U.S. part of the Sunda Strait observation is supported by the Office of Naval Research, USA, grant # N00014-08-01-0618. All in situ data are archived at the Agency for Marine and Fisheries Research and Human Resources. The processed data are available from the authors upon request (weizx@fio.org.cn). The sea level anomaly data were produced by Ssalto/Duacs and distributed by AVISO (http://www.aviso.altimetry.fr/duacs/). CCMP version 2.0 vector wind analyses were produced by Remote Sensing Systems (http://www.remss.com).

## References

Atlas R, Hoffman RN, Ardizzone J et al (2011) A cross-calibrated, multiplatform ocean surface wind velocity product for meteorological and oceanographic applications. Bull Am Meteorol Soc 92:157–174

Dharma A, Murray SP (1996) Low-frequency fluctuations in the Indonesian Throughflow through Lombok Strait. J Geophys Res 1011:12455–12464

Drushka K, Sprintall J, Gille ST et al (2010) Vertical structure of Kelvin waves in the Indonesian Throughflow exit passages. J Phys Oceanogr 40:1965–1987

Ducet N, Traon PY, Reverdin G (2000) Global high resolution mapping of ocean circulation from the combination of TOPEX/POSEIDON and ERS-1/2. J Geophys Res 105(C8):19477–19498

Fang G, Susanto RD, Wirasantosa S et al (2010) Volume, heat and freshwater transports from the South China Sea to Indonesian Seas in the boreal winter of 2007-2008. J Geophys Res 115:93–102

Gordon AL, Sprintall J, Van Aken H et al (2010) The Indonesian Throughflow during 2004–2006 as observed by the INSTANT program. Dyn Atmos Oceans 50:115–128

Iskandar I, Mardiansyah W, Masumoto Y et al (2005) Intraseasonal Kelvin waves along the southern coast of Sumatra and Java. J Geophys Res 110:169–189

Iskandar I, Masumoto Y, Mizuno K et al (2014) Coherent intraseasonal oceanic variations in the eastern equatorial Indian Ocean and in the Lombok and Ombai Straits from observations and a high-resolution OGCM. J Geophys Res Oceans 119:615–630

Madden RA, Julian PR (1994) Observations of the 40-50-day tropical oscillation: a review. Mon Weather Rev 122:814–837

Molcard R, Fieux M, Ilahude AG (1996) The Indo-Pacific throughflow in the timor passage. J Geophys Res 101:12411–12420

Pujiana K, Gordon AL, Sprintall J (2013) Intraseasonal Kelvin wave in Makassar Strait. J Geophys Res Oceans 118:2023–2034

Roundy PE, Kiladis GN (2006) Observed relationships between oceanic Kelvin waves and atmospheric forcing. J Climate 19:5253–5272

Schiller A, Wijffels SE, Sprintall J et al (2010) Pathways of intraseasonal variability in the Indonesian Throughflow region. Dyn Atmos Oceans 50:174–200

Sprintall J, Wijffels SE, Molcard R et al (2009) Direct estimates of the Indonesian Throughflow entering the Indian Ocean: 2004–2006. J Geophys Res 114:358–368

Susanto RD, Gordon AL, Sprintall J et al (2000) Intraseasonal variability and tides in Makassar strait. Geophys Res Lett 27:1499–1502

Susanto RD, Wei Z, Adi TR et al (2013) Observations of the Karimata throughflow from December 2007 to November 2008. Acta Oceanol Sin 32:1–6

Susanto RD, Wei Z, Adi TR et al (2016) Oceanography surrounding Krakatau Volcano in the Sunda Strait, Indonesia. Oceanography 29:264–272

Wei Z, Fang G, Susanto RD et al (2016) Tidal elevation, current and energy flux in the area between the South China Sea and Java Sea. Ocean Sci Discuss 12:517–531

Wijffels S, Meyers G (2004) An intersection of oceanic waveguides: variability in the Indonesian Throughflow region. J Phys Oceanogr 34:1232–1253

Wu Z, Huang NE (2009) Ensemble empirical mode decomposition: a noise-assisted data analysis method. Adv Adapt Data Anal 1:1–41

Xu T, Wei Z, Cao G et al (2016) Pathways of Intraseasonal Kelvin waves in the Indonesian Throughflow regions derived from satellite altimeter observation. Atmos Ocean Sci Lett 9:375–380

Zhou L, Murtugudde R (2010) Influences of Madden–Julian oscillations on the eastern Indian Ocean and the maritime continent. Dyn Atmos Oceans 50:257–274